Available online at www.sciencedirect.com
ScienceDirect
Journal of the European Ceramic Society 28 (2008) 1623–1629
www.elsevier.com/locate/jeurceramsoc

Preparation of Ni(II)/Ti(IV) layered double hydroxide at high supersaturation

W.H. Zhang, X.D. Guo, J. He *, Z.Y. Qian

State Key Laboratory of Chemical Resource Engineering, Beijing University of Chemical Technology, Beijing 100029, PR China

Received 2 February 2007; received in revised form 1 November 2007; accepted 25 November 2007
Available online 19 February 2008

Abstract

Ni(II)/Ti(IV) carbonate layered double hydroxide with high crystallinity has been synthesized by high supersaturation method. The structure and chemical composition of the compound have been characterized by PXRD, FT-IR, ICP-AES, SEM, N_2 adsorption–desorption isotherms, UV–vis, TG–DTA, and in situ HT-XRD techniques. It is found that Ti(IV) ions are incorporated into the brucite-like layer and the high positive charge of the layers has no obvious effect on the basal spacing. But the substitution of Ti(IV) for Ni(II) in the layer decreases the thermal stability of the resulting LDH materials.

Keywords: Layered double hydroxide; Coprecipitation; Formation mechanism; Ni–Ti–CO_3; Thermal stability

1. Introduction

Layered double hydroxides (LDHs), also called hydrotalcite-like compounds, are a big family of promising materials that can be used as catalysts,[1] catalyst supports,[2] ion exchangers[3] and additives.[4] The general formula of these compounds is $[M^{2+}_{1-x}M^{3+}_{x}(OH)_2]A^{n-}_{x/n}\cdot yH_2O$, where M^{2+} and M^{3+} represent divalent and trivalent cations, respectively, and A^{n-} is the charged balancing anions. The structure of these materials consists of brucite-like layer in which a part of M^{2+} is replaced isomorphously by M^{3+}, so the excess positive charge of the layer is compensate by anions between the layers, and water molecules may occupy the remaining space of the interlayer region. In addition to divalent and trivalent cations, a wide range of cations such as Li^+, Sn^{4+}, Zr^{4+}, Ti^{4+}, etc.[5–8] may be accommodated in the octahedral sites of close-packed configuration of OH^- ions in the layers of these compounds.

Ti containing LDHs have received much attention for their potential application for removal toxic anionic substances from industry wastewater,[8] and are supposed to be potential catalysts for the transformation of organic molecules in liquid phase reactions, similar to Ti containing zeolites.[9] Zn–Ti and Co–Ti LDH have been synthesized by urea method.[10–12] Considering nickel is a more important element for catalysis and electrochemistry than other transition metals,[13] our group recently is engaged in the synthesis of Ni–Ti LDH.[14] During the synthesis process, decomposition of urea releases ammonia and carbonate ions in a uniform fashion, resulting in a gradual and uniform increase in the pH of the solution, and leading to a low degree of supersaturation during precipitation and a decrease in the nucleation rate. Usually, urea hydrolysis can be applied to the preparation of well-crystallized LDHs. But, for Ni–Ti LDH, poor crystallization was obtained which shows asymmetric and broadening reflection on the high angle region of XRD patterns.[14] Since the decomposition of urea and nucleation process for urea method needs a high temperature, urea method is unfavorable for unstable metal hydroxide such as titanium hydroxide and liable to produce materials with less crystallinity. In this paper, high supersaturation method is chosen to synthesize Ni–Ti–CO_3 LDH with high crystallinity, in which nucleation process is performed under ambient conditions.[15] The structure, properties and the formation mechanism of the Ni–Ti–CO_3 LDH have been investigated.

* Corresponding author. Tel.: +86 10 64425280; fax: +86 10 64425385.
E-mail address: jinghe@263.net.cn (J. He).

0955-2219/$ – see front matter © 2008 Elsevier Ltd. All rights reserved.
doi:10.1016/j.jeurceramsoc.2007.11.016

2. Experimental

2.1. Preparation

The Ni–Ti–CO_3 LDH was prepared by high supersaturation method similar to the synthesis of Mg–Al LDH.[16] A solution of NaOH [molar ratio: NaOH/(Ni^{2+} + Ti^{4+}) = 1.75] and Na_2CO_3 (molar ratio: Na_2CO_3/Ti^{4+} = 2.2) was added dropwise to a vigorous stirred solution of $Ni(NO_3)_2{\cdot}6H_2O$ and $Ti(SO_4)_2$ with different Ni/Ti ratios until the pH reached 9.5 under room temperature. The resulting suspension was aged at a refluxing temperature for 6 h. The mixture was filtered and the solid washed thoroughly with deionized water and dried at 70 °C for 12 h.

The hydrothermal aging experiments were performed as follows. The suspension obtained after just completion of adding NaOH and Na_2CO_3 mixture solution to $Ni(NO_3)_2{\cdot}6H_2O$ and $Ti(SO_4)_2$ solution was placed in an autoclave, hydrothermally treated at 100 or 150 °C for 6 h. The solid was collected by filtration, washed with deionized water thoroughly, and dried at 70 °C for 12 h.

For comparison, Ni–Ti LDH is also prepared by urea method according to literature.[14] A solution of $TiCl_4$ prepared through $TiCl_4$ and HCl with volume ratio 1:1, $Ni(NO_3)_2{\cdot}6H_2O$ and urea were added to deionized water under vigorous stirring. The resulting solution was stirred for 6 h at refluxing condition. The filter cake was washed twice with deionized water, once with anhydrous ethanol, and dried overnight at 60 °C.

2.2. Characterization

Powder XRD patterns of the samples were obtained using a Shimadzu XRD-6000 diffractometer (Cu Kα radiation, step size of 0.02°, scan speed of 5°/min). Elemental analysis for Ni and Ti was carried out using inductively coupled plasma emission spectroscopy (Shimadzu ICPS-7500). Solid state UV–vis diffuse reflectance spectra were recorded at room temperature and in air by means of a UV-2501PC spectrometer equipped with an integrating sphere attachment using $BaSO_4$ as background. FT-IR spectra were recorded on a Bruker Vector 22 FT-IR spectrometer (resolution 4 cm^{-1}), the samples being pressed into KBr discs with a weight ratio of sample to KBr of 1:100. The low-temperature N_2 adsorption–desorption experiments were carried out using a Quantachrome Autosorb-1 system. The samples were degassed for 4 h at 70 °C before the analysis. The specific surface area was calculated using the BET method based on the absorption isotherm and pore size distribution was calculated using the BJH method based on the desorption isotherm. Scanning electron microscopy (SEM) was performed with HITACHI S-4300. Thermal analyses were carried out on a PCT-IA thermal analysis system in air with a temperature increase of 10 °C/min. In situ HT-XRD measurements were performed on a Shimadzu XRD-6000 diffractometer in air, using Cu Kα radiation (λ = 0.154 nm). The samples as un-oriented powders were scanned in steps of 0.05° in the range 3–70° using a count time of 6 s per step.

3. Results and discussion

3.1. Structure and properties of Ni(II)/Ti(IV) LDH

Ni–Ti–CO_3 LDHs with various atomic ratios were synthesized using high supersaturation method and the resulting solids were characterized by PXRD, as shown in Fig. 1. Ni:Ti atomic ratios are altered from 2:1 to 5:1 (denominated as samples A–D, respectively) and sample B (Ni:Ti = 3:1) exhibits higher crystalline LDH phase. Except the sample B, PXRD of other samples show very weak diffraction peaks corresponding to β-nickel hydroxide. So, our study and presentation will be restricted to the sample B.

The powder X-ray diffraction of the sample B shows basal peaks corresponding to (0 0 3), (0 0 6) and (0 0 9) and non-basal peaks attributed to (0 1 2), (0 1 5), (0 1 8), (1 1 0) and (1 1 2) reflections, as shown in Fig. 1b. The peaks exhibit the common features of layered materials such as narrow, symmetric and strong peaks at low 2θ (°) as well as weaker and less symmetric peaks at high 2θ values. The absence of the (h 0 l) non-basal peaks indicates the turbostratic effect on the sample caused by the decease in the order along the stacking axis. The basal interlayer spacing of Ni–Ti–CO_3 LDH is 0.775 nm calculated from (0 0 3) reflection, similar to that of Ni–Al–CO_3 LDH.[17] Although Ni–Ti–CO_3 LDH has higher charge density than Ni–Al–CO_3 LDH, the gallery height equals the carbonate anion size because of the Van der Waals repulsion between hydroxide of the layer and carbonate inhibits the decrease of the interlayer space. For the sample with the PXRD peaks intense and sharp enough for accurate determination, the crystallographic parameters are evaluated assuming rhombohedral symmetry (space group $R3m$). The lattice parameters 'a' is 0.308 nm calculated from (1 1 0) reflection, and the lattice parameters 'c' is 2.325 nm calculated from (0 0 3) reflection, respectively, for as-synthesized sample B. The lattice parameters 'a' and 'c' were reported to be 0.304 and 2.317 nm for Ni–Al–CO_3 LDH.[17] The lattice parameters 'a' represents the distance of cations in the layer, so the cation distance in the layer of Ni–Ti–CO_3 LDH is

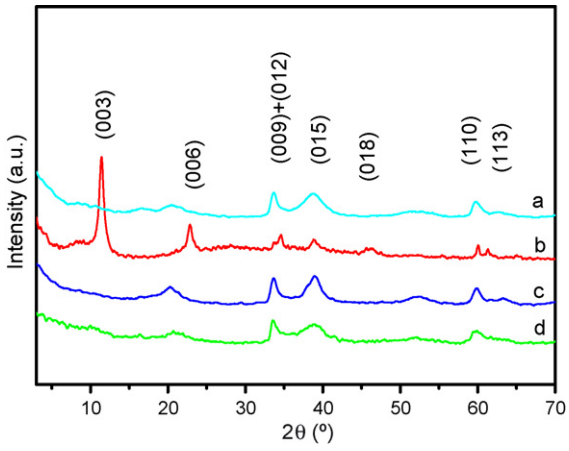

Fig. 1. Powder X-ray diffraction patterns of Ni–Ti LDH synthesized by high supersaturation method with different Ni and Ti atomic ratio: (a) Ni/Ti = 2, (b) Ni/Ti = 3, (c) Ni/Ti = 4, and (d) Ni/Ti = 5.

larger than that of Ni–Al–CO_3 LDH which could be attributed to the larger ion radii of Ti^{4+} than that of Al^{3+}(0.068 nm *versus* 0.054 nm). The lattice parameter '*c*' corresponds to the triple of the sum of the thickness of one brucite-like layer and one gallery height. The lattice parameter '*c*' of sample B is similar to Ni–Al–CO_3 LDH, but different from that of the Ni (II)/Ti(IV) LDH synthesized by the urea method[14] because their anions of the LDH interlayer are carbonate and cyanate, respectively.

ICP-AES analysis for this sample shows that the Ni/Ti mole ratio is 2.74, slightly lower than the molar ratio existing in the starting solution. This phenomenon is rather common and may be ascribed to a preferential precipitation of one cation as hydroxide.[10]

UV–vis diffuse reflectance spectroscopy only exhibits an adsorption band near 537 nm attributed to charge transfer involving Ni^{2+} species, as shown in Fig. 2. No bands around 220 and 320 nm are observed, which are characteristic of pure TiO_2,[18] clearly demonstrating the absence of any TiO_2 species. This also indicates that Ti^{4+} ion has isomorphously substituted for Ni^{2+} in the brucite-like layer, although it has high valence and strong electronegativity.

FT-IR spectroscopy is used to identify the nature and symmetry of interlayer anions. The FT-IR spectrum of Ni–Ti–CO_3 LDH, illustrated in Fig. 3, shows a strong band centered around 3442 cm^{-1} that is ascribed to a superposition of the OH stretching mode of layer hydroxyl groups and hydrogen-bonded interlayer water molecules. For Ni–Al LDH, this band appears around 3500 cm^{-1}.[19] The shift of OH stretching mode of layer hydroxyl groups to low frequency is probably caused by the electron density on the O–H bond modified by Ti^{4+} electro-negativity. The extreme broadness of the OH band is owed to the presence of hydrogen bonding between hydroxides of layers, interlayer water and anions in the interlayer gap.[19] A low-resolution band around 1630 cm^{-1} ascribed to the bending mode of water molecules indicates a small amount of interlayer water in Ni–Ti LDH due to abundant anions compensated positive charge of the layer. For carbonate LDH which consists of M(II) and M(III), interlayer carbonate anions are symmetrically hydrogen-bonded to water molecules. Only a single band is observed at 1370 cm^{-1}, which means that the symmetry of carbonate anions is close to free anions, *i.e.*, D_{3h} symmetry.[20] For Ni–Ti–CO_3 however, this band is splitted to two ones located at 1509 and 1384 cm^{-1}. The splitting is probably due to the restricted symmetry in the interlayer space. Ti^{4+} cations incorporated in the brucite-like layer bring two valence positive charges, so the electrostatic attraction between the layer and the interlayer carbonate anions is stronger than that in Ni–Al–CO_3 LDH, influencing the symmetries of the interlayer anions. The symmetries of the carbonate anions decreased from D_{3h} of free anions to C_{2v} due to the disordered nature of the interlayer space, as observed previously.[20] The weak band at 1126 cm^{-1} for Ni–Ti LDH can be ascribed to the bending mode of carbonate ions. The band at 635 cm^{-1} is attributed to the overlap of the asymmetric vibration of CO_3^{2-} and M–O stretching vibrations.

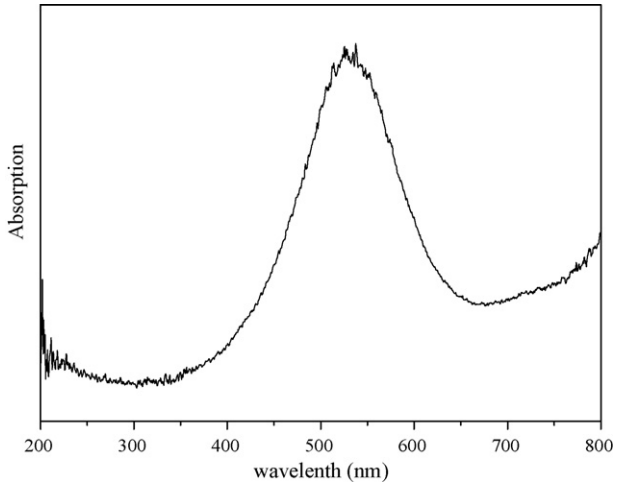

Fig. 2. Solid state UV–vis diffuse reflectance spectrum of Ni–Ti–CO_3 LDH (Ni/Ti = 3).

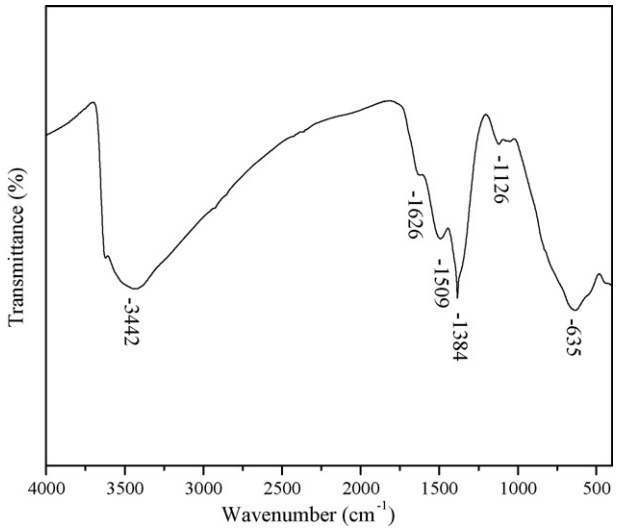

Fig. 3. FT-IR spectrum of Ni–Ti–CO_3 LDH (Ni/Ti = 3).

Low temperature N_2 adsorption–desorption isotherm of Ni–Ti–CO_3, illustrated in Fig. 4, shows a type II isotherm due to capillary condensation in mesopores where adsorption is limited for high relative pressure.[21] The isotherm is found to exhibit H3 type hysteresis loop characteristic of pores with narrow necks, which is associated with aggregates of plate-like particles giving rise to slit-shaped pores. The specific surface area of the Ni–Ti–CO_3 LDH determined by BET method is 37 $m^2\ g^{-1}$, the modal pore diameter is around 4 nm, and the total pore volume is 0.11 $cm^3\ g^{-1}$, similar to Mg–Al LDH by Yun and Pinnavaia,[22] but smaller than Ni–Ti–cyanate LDH[14] due to different preparation procedure. This means that the agglomeration of Ni–Ti LDH obtained by high supersaturation method is more severe than Ni–Ti LDH prepared by urea method. The specific surface area of non-aged Ni–Ti–CO_3 LDH is ca. 2 $m^2\ g^{-1}$, due to severe aggregation of the LDH microcrystals, as observed for Mg–Al LDH.[23]

SEM image of Ni–Ti–CO_3 LDH, shown in Fig. 5, reveals that Ni–Ti LDH shows no characteristic "sand-rose" morphology while plate-like particles with irregular size are stacking with each other. The Ni–Ti LDH plates are below 100 nm in the lateral

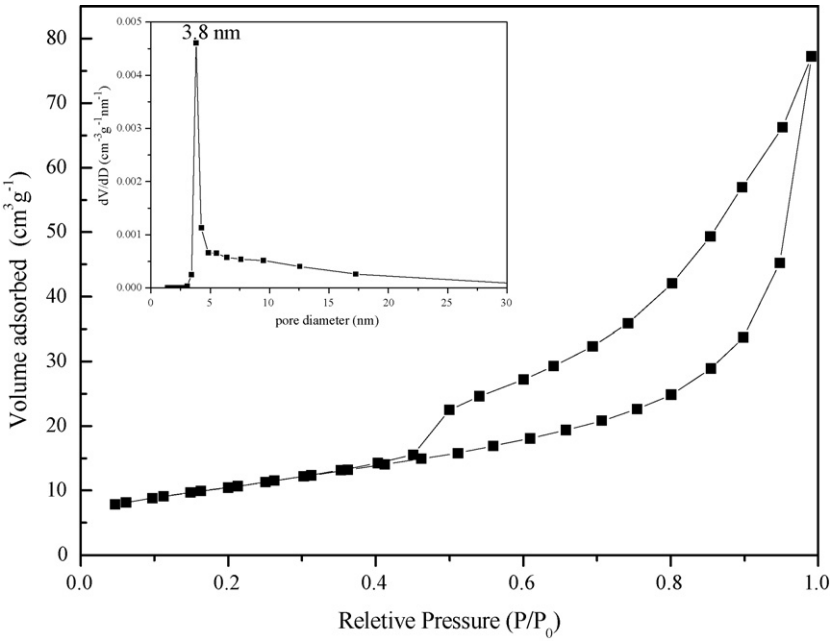

Fig. 4. N_2 adsorption–desorption isotherms and pore size distribution (inset) of Ni–Ti–CO_3 LDH (Ni/Ti = 3).

dimension, smaller than general observed LDH which are sized in hundreds of nanometer. Small LDH plates agglomerate to form large particle ca. several micrometer.

TG–DTA curve for Ni–Ti–CO_3 LDH is shown in Fig. 6. The TG curve exhibits two weight loss steps as well as two endothermic DTA peak and the total weight loss is 24.6%. The first one (31–199 °C, 7.5%) is due to the loss of both adsorbed and interlayer water, in the meantime the partial dehydroxylation of the layer also occurs, corresponding to the endothermic DTA peak at 128 °C. The second step (199–700 °C, 17.1%) is a consequence of complete dehydroxylation of the layer and loss of carbonate in the interlayer region corresponding to the endothermic DTA peak at 272 °C. The second one shifts to low temperature in comparison with Ni–Al–CO_3 which has the corresponding endothermic DTA peak at 355 °C,[24] indicating that Ni–Ti LDH can be decomposed more easily upon thermal treatment due to the presence of Ti^{4+} in the host layers. Compared with Al^{3+}, the high electronegative Ti^{4+} can easily accept the oxygen of both water molecule and carbonate anion.

In situ HT-XRD patterns of Ni–Ti–CO_3 LDH sample recorded in the temperature range of 25–600 °C are shown in Fig. 7. This technique gives substantial information on the different phases during decomposition process. Upon the heating of the sample from 25 to 150 °C, the reflection of the d_{003} basal spacing shifts slightly from 0.775 to 0.559 nm, corresponding to the removal of interlayer water as observed in TG–DTA. If the layer thickness is 0.48 nm similar to Zn–Al LDH,[25] the gallery height is 0.179 nm calculated by the basal spacing subtracted the layer thickness, which is smaller than the size of carbonate anions (0.28 nm). This indicates that the carbonate has been grafted to the layer. Similar behavior is already reported for Ni–Fe–CO_3 LDH.[26] Meanwhile, the (1 1 3) reflection vanishes, while the intensity of the (1 1 0) reflection diminishes

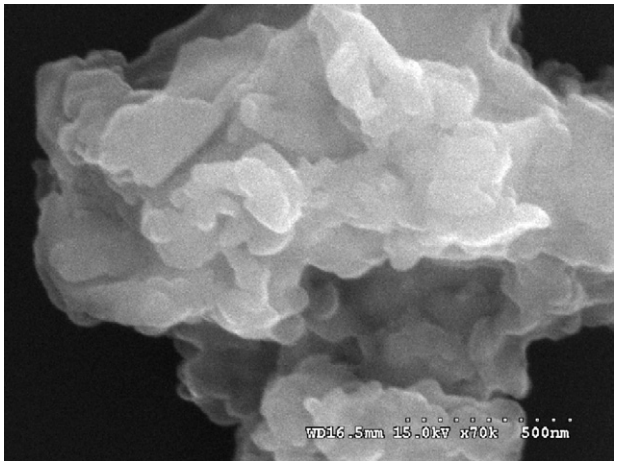

Fig. 5. SEM micrograph of Ni–Ti–CO_3 LDH (Ni/Ti = 3).

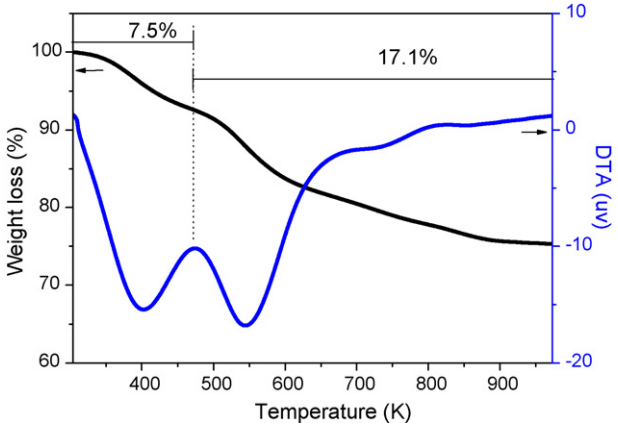

Fig. 6. TG and DTA curves of Ni–Ti–CO_3 LDH (Ni/Ti = 3).

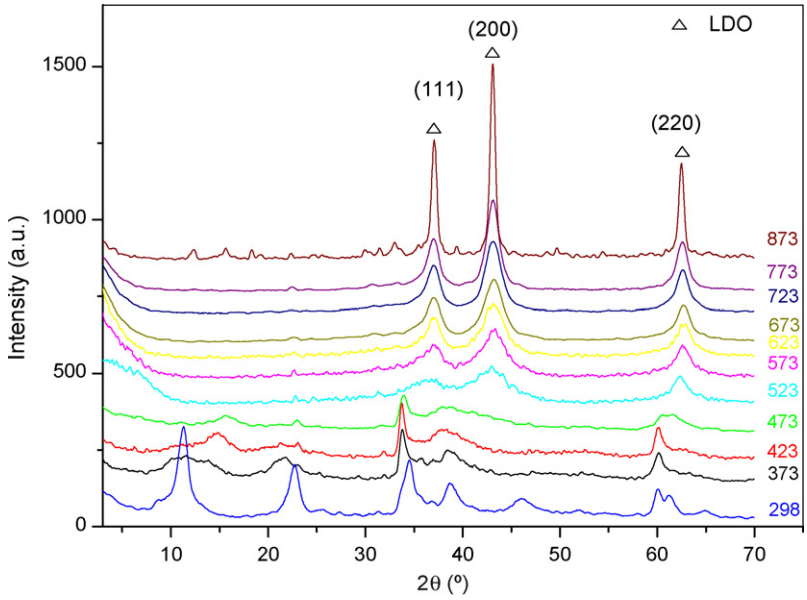

Fig. 7. In situ HT-XRD patterns of Ni–Ti–CO_3 LDH (Ni/Ti = 3) in the temperature range 25–600 °C.

significantly, becoming broader. The diffraction peaks of layered double hydroxide disappear above 250 °C due to the dehydroxylation of the layer and remove of CO_2 from the interlayer, as observed at 274 °C in TG–DTA, which means the layered double hydroxide structure is collapsed. The reflection of the layered double oxide (LDO) phase appears at 250 °C and becomes more sharp and symmetric with increasing temperature, which is similar to NiO Phase (JCPDS File No. 44-1159). No TiO_2 phase observed shows that Ti^{4+} is dispersed in NiO rocksalt phase as a solid solution. The formation of solid solution is also observed during the thermal decomposition of Mg–Al LDH.[27]

3.2. The influences factors of Ni–Ti LDH formation

As discussed above, the samples with various atomic ratios were synthesized using high supersaturation method and the resulting solids were characterized by PXRD. The high crystalline LDH phase is observed only for the sample with Ni:Ti = 3:1. Although most LDHs materials can be synthesized in the range of metal ratio 5:1 to 2:1,[16] the Ni–Ti–CO_3 LDH synthesized by high supersaturation method is an exception in this case, because Ti^{4+} ion has higher valence and higher polarization which is difficult for its substitution of Ni^{2+} in the brucite-like layer. So the formation of Ni–Ti LDH is sensitive to the preparation method applied.

It is worthwhile to note that Ni–Ti LDH could be synthesized while the metal ratio ranges from 5:1 to 1.5:1 using $TiCl_4$ as Ti source by urea method.[14] Usually, the urea method can obtain LDH with higher crystallinity[15] than high supersatuation method, but for the synthesis of Ni–Ti LDH, low crystalline LDH phase was obtained as showed in Fig. 8a which has a *d*-spacing value of 0.73 nm corresponding to cyanate LDH, consistent with reported previously by our group.[14] When $Ti(SO_4)_2$ was used as Ti source, the amorphous sediment was obtained as shown in Fig. 8b. Obviously the Ti source has important effect on the formation of the Ni–Ti LDH. In the urea method, the nucleation temperature of Ni(II)/Ti(IV) LDH is 100 °C, so Ti^{4+} cation is easily precipitated to amorphous oxide under high temperature condition. The anions in the Ti source present in solution can affect the solubility of the amorphous titanium oxide which is critical to the formation of Ni(II)/Ti(IV) LDH. Chloride ions can promote effectively the dissolve of Ti^{4+} ions because they form stronger complex with Ti^{4+} than sulfate ions. In high supersaturation method, however, the titanium oxide with higher soluble ability is ready to form because the nucleation process occurred at ambient temperature, lower than that in urea method, resulting in a higher crystallized Ni–Ti–CO_3 (Fig. 1b) even using $Ti(SO_4)_2$ as Ti source. Therefore, both $Ti(SO_4)_2$ and $TiCl_4$ are suitable for the formation Ni(II)/Ti(IV) LDH in this method.

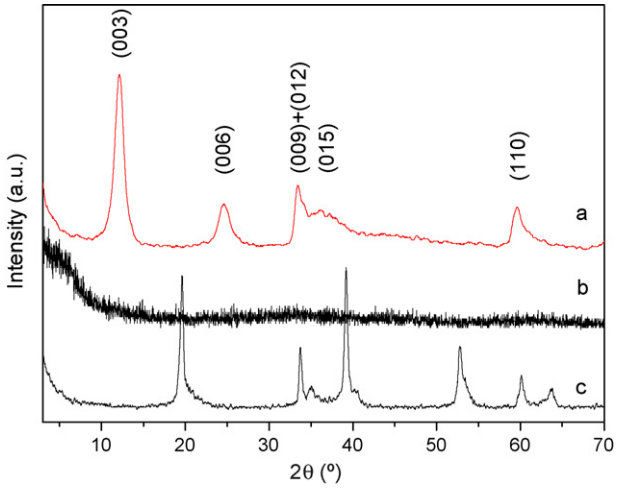

Fig. 8. Powder X-ray diffraction patterns of Ni–Ti LDH (Ni/Ti = 3 in the synthesis mixture) synthesized in different conditions: (a) urea method using $TiCl_4$ as Ti source, (b) urea method using $Ti(SO_4)_2$ as Ti source, and (c) high supersaturation method with hydrothermal treatment, using $Ti(SO_4)_2$ as Ti source.

$Ti(SO_4)_2$ is convenient compared with $TiCl_4$, so it is useful for practical application.

Aging temperature also has important effects on the crystallinity of the samples. The aging temperature suitable for the formation of Ni–Ti LDH phase is 100 °C in refluxing condition. On this aging temperature, the similar crystallinity is obtained for the Ni–Ti LDH samples treated under refluxing condition and in hydrothermal condition respectively. When the aging temperature in hydrothermal condition is increased to 150 °C, only β-$Ni(OH)_2$ phase (Fig. 8c) is obtained, and no XRD peaks corresponding to TiO_2 phase are observed due to Ti^{4+} existing as amorphous hydrous oxide materials. For Mg–Al LDH, the high temperature is benefit to the crystallization process.[16] But, for the formation of the Ni–Ti LDH structure, the low synthetic temperature is required. This indicates that Ni–Ti–CO_3 LDH has low thermal stability, also observed in TG–DTA.

The study on the aging time shows that the preferable aging time is 6 h under both refluxing and hydrothermal treatment, and the low crystalline sample was obtained before 6 h and phase transformation occurred after 6 h.

3.3. Formation mechanism of Ni–Ti LDH

Although a large number of LDH materials have been synthesized and studied, their formation mechanisms are still far from clear.[28–33] Many formation mechanisms have been proposed, such as the topotactical mechanism for reconstruction from calcined Mg–Al LDH system,[28–30] dissolution-crystallization for Mg–Al salt system,[31] one-step formation mechanism for Zn–Cr salt system,[32] and dissolution–deposition–diffusion mechanism for Al_2O_3–MgO system.[33]

To investigate Ni–Ti LDH formation process, a titration behavior of $Ni(NO_3)_3$ (aq), $Ti(SO_4)_2$ (aq) and their mixed solution with a molar ratio of Ni^{2+} to Ti^{4+} as 3:1 against alkaline solution was investigated respectively, as shown in Fig. 9. Each one single metal salt solution yields one pH plateau corresponding to the precipitation of their respective hydroxides. However, the mixed metal salt solution yields two pH plateau, the value of the second plateau is different from that of corresponding single metal salt solution. The first plateau at pH value of 1.8 is identical to that of single $Ti(SO_4)_4$ solution (Fig. 9b), corresponding to the formation of titanium hydroxide. The second plateau at pH value of 7.4 is obviously lower than that of only Ni^{2+} solution (pH 7.7) (Fig. 9a).

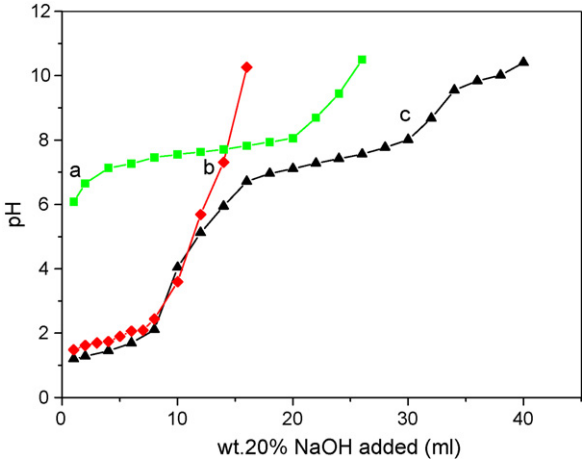

Fig. 9. Titration curves of (a) $Ni(NO_3)_2$ solutions, (b) $Ti(SO_4)_2$ solutions, and (c) mixture solution of $Ni(NO_3)_2$ and $Ti(SO_4)_2$ in a Ni/Ti of 3:1.

According to the titration curves above, we suggest that the Ti^{4+} ions precipitate as titanium hydroxide in preference to Ni^{2+} ions on the first plateau. When pH increases to the second plateau, Ni–Ti LDH is formed by Ni^{2+} ions and Ti^{4+} ions in the solution. Ti ions can be continuously supplied by the dissolution of titanium hydroxide precipitated previously when the Ti^{4+} ions in solution is depleted because of formation of Ni–Ti LDH. The formation of Ni–Ti LDH is processed through the solid dissolution, so this process is slower than a simple precipitation of solution. Due to this reason, it is observed during titration process that a constant pH was reached within 10 min after each addition of hydroxide in the second plateau but the corresponding time in the first plateau is within half of minute. This phenomenon is also attributed to the formation of Ni–Ti LDH.

The process of formation of Ni–Ti LDH can be explained by the complete precipitation of $Ti(OH)_4$ firstly, followed by its transformation to the layered double hydroxide with Ni^{2+} ions and anions. Therefore, the whole reaction can be expressed as this interpretation:

$$Ti(OH)_4 + 3Ni^{2+}{}_{(aq)} + 6OH^- + {CO_3}^{2-} \rightleftharpoons Ni_3Ti(OH)_8CO_3 \quad (1)$$

The reverse process of the above reaction is the dissolution of Ni–Ti LDH, so a nominal K_{sp} for Ni–Ti LDH may be inferred from the expression:

$$K_{sp,LDH} = K_{sp,Ti(OH)_4}[Ni^{2+}]^3[OH^-]^6[{CO_3}^{2-}] \quad (2)$$

From the titration curves, we can calculated solubility product constants for the Ni–Ti LDH, $Ni(OH)_2$ and $Ti(OH)_4$. Then the values of pK_{sp} are 93.0, 13.5 and 50.3, respectively. For the overall process, the formation of LDH can be expressed by the reaction in which a mixture of simple hydroxides is converted to LDH:

$$Ti(OH)_4 + 3Ni(OH)_2 + {CO_3}^{2-} = Ni_3Ti(OH)_8CO_3 + 2OH^- \quad (3)$$

The equilibrium constant for this reaction is given by

$$pK_{convertion} = pK_{sp,LDH} - pK_{sp,Ti(OH)_4} - 3pK_{sp,\ Ni(OH)_2} \quad (4)$$

So the value of p$K_{convertion}$ is 2.2, which indicates that the relative stability of Ni–Ti LDH is higher than that of a simple mixture of $Ti(OH)_4$ and $Ni(OH)_2$.

Because the formation process of Ni–Ti LDH is combined with Ti^{4+} ions dissolution from titanium hydroxide precipitated in the first pH plateau, this process could be regarded as dissolution-crystallization mechanism, similar mechanism is proposed for Mg–Al LDH, Mn–Al LDH and Mg–Fe LDH.[31] The formation of the LDH structure takes place at a pH value lower than that for $Ni(OH)_2$ formation, meaning higher stability

of Ni–Ti LDH in comparison with $Ni(OH)_2$. When the titration was completed, a weak crystalline LDH phase was observed. Then, through the subsequent aging process, it can be converted to a well-crystallized LDH.

4. Conclusions

In this study, Ni–Ti–CO_3 LDH was prepared by high supersaturation method. Ti (IV) ions are incorporated in the host layers, and no extra-framework titanium species exist in the Ni–Ti LDH. The formation of Ni–Ti LDH structure is explained according to the dissolution-crystallization mechanism at this condition. The interlayer carbonate anions display C2v symmetry duo to interlayer confinement effect. The thermal stability of Ni–Ti–CO_3 LDH is lower than the general LDH counterparts, because Ti(IV) has strong electronegativity. A further aim is to investigate the application of Ni–Ti LDH in catalysis field.

Acknowledgements

The authors are grateful to the financial support from NSFC (20473008 and Key Project: 20531010), Ministry of Education (20050010007, IRT0406) and Program for New Century Excellent Talents in University (NCET-04-0119).

References

1. Reichle, W. T., Catalytic reactions by thermally activated, synthetic, anionic clay minerals. *J. Catal.*, 1985, **94**(2), 547–557.
2. Gardner, E. A., Yun, S. K., Kwon, T. and Pinnavaia, T. J., Layered double hydroxides pillared by macropolyomexalates. *Appl. Clay Sci.*, 1998, **13**, 479–494.
3. Sasaki, S., Aisawa, S., Hirahara, H., Sasaki, A., Nakayama, H. and Eiichi, N., Synthesis of *p*-sulfonated calix[4]arene-intercalated layered double hydroxides and their adsorption properties for organic molecules. *J. Eur. Ceram. Soc.*, 2006, **26**, 655–659.
4. Evans, D. G. and Duan, X., Preparation of layered double hydroxides and their applications as additives in polymers, as precursors to magnetic materials and in biology and medicine. *Chem. Commun.*, 2006, **6**(5), 485–496.
5. Chisem, I. C. and Jones, W., Ion-exchange properties of lithium aluminium layered double hydroxides. *J. Mater. Chem.*, 1994, **4**(11), 1737–1744.
6. Velu, S., Suzuki, K. and Osaki, T., A comparative study of reactions of methanol over catalysts derived from NiAl- and CoAl-layered double hydroxides and their Sn-containing analogues. *Catal. Lett.*, 2000, **69**, 43–50.
7. Velu, S., Ramaswamy, V., Ramani, A., Chanda, B. M. and Sivasanker, S., New hydrotalcite-like anionic clays containing Zr^{4+} in the layers. *Chem. Commun.*, 1997, 2107–2108.
8. Das, N. and Samal, A., Synthesis, characterization and rehydration behaviour of titanium(IV) containing hydrotalcite like compounds. *Micropor. Mesopor. Mater.*, 2004, **72**, 219–225.
9. Adam, W., Corma, A., García, H. and Weichold, O., Titanium-catalyzed heterogeneous oxidations of silanes, chiral allylic alcohols, 3-alkylcyclohexanes, and thianthrene 5-oxide: a comparison of the reactivities and selectivities for the large-pore zeolite Ti-β, the mesoporous Ti-MCM-41, and the layered aluminosilicate Ti-ITQ-2. *J. Catal.*, 2000, **196**(2), 339–344.
10. Saber, O. and Tagaya, H., New layered double hydroxide, Zn-Ti LDH: preparation and intercalation reactions. *J. Incl. Phenom. Macropro.*, 2003, **45**, 109–116.
11. Saber, O. and Tagaya, H., Preparation of new layered double hydroxide, Co–Ti LDH. *J. Incl. Phenom. Macropro.*, 2005, **51**, 17–25.
12. Saber, O., Hatano, B. and Tagaya, H., Controlling of the morphology of Co–Ti LDH. *Mater. Sci. Eng.*, 2005, **25**, 462–471.
13. Zilbermann, I., Maimon, E., Cohen, H. and Meyerstein, D., Redox chemistry of nickel complexes in aqueous solutions. *Chem. Rev.*, 2005, **105**, 2609–2626.
14. Shu, X., Zhang, W. H., He, J., Gao, F. X. and Zhu, Y. X., Formation of Ni–Ti layered double hydroxides using homogeneous precipitation method. *Solid. State. Sci.*, 2006, **8**, 634–639.
15. He, J., Wei, M., Li, B., Kang, Y., Evans, D. G. and Duan, X., Preparation of layered double hydroxides. *Struct. Bond.*, 2006, **119**, 89–119.
16. Cavani, F., Trifiro, F. and Vaccari, A., Hydrotalcite-type anionic clays: preparation, properties and applications. *Catal. Today*, 1991, **11**, 173–301.
17. Cailerie, J. B. D., Kermarec, M. and Clause, O., Impregnation of gamma-alumina with Ni(II) or Co(II) ions at neutral pH: hydrotalcite-type coprecipitate formation and characterization. *J. Am. Chem. Soc.*, 1995, **117**, 11471–11481.
18. He, J., Guo, Z., Ma, H., Evans, D. G. and Duan, X., Enhancing the selectivity of benzene hydroxylation by tailoring the chemical affinity of the MCM-41 catalyst surface for the reactive molecules. *J. Catal.*, 2002, **212**, 22–32.
19. Ehlsissen, K. T., Delahaye-Vidal, A., Genin, P., Figlarz, M. and Willmann, P., Preparation and characterization of turbostratic Ni/Al layered double hydroxides for nickel hydroxide electrode applications. *J. Mater. Chem.*, 1993, **3**, 883–888.
20. Hernandez-Moreno, M. J., Ulibarri, M. A., Rendon, J. L. and Serna, C. J., IR characteristics of hydrotalcite-like compounds. *Phys. Chem. Miner.*, 1985, **12**, 34–38.
21. Sing, K. S. W., Everett, D. H., Haul, R. A. W., Moscou, L., Pierotti, R., Rouquerol, J. and Sieminiewska, T., Reporting physisorption data for gas/solid systems with special reference to the determination of surface area and porosity. *Pure Appl. Chem.*, 1985, **57**, 603–619.
22. Yun, S. K. and Pinnavaia, T. J., Water content and particle texture of synthetic hydrotalcite-like layered double hydroxides. *Chem. Mater.*, 1995, **7**, 348–354.
23. Albiston, L., Franklin, K. R., Lee, E. and Smeulder, J. B. A. F., Rheology and microstructure of aqueous layered double hydroxide dispersions. *J. Mater. Chem.*, 1996, **6**, 871–877.
24. Jitianu, M., Balasoiu, M., Zaharescu, M., Jitianu, A. and Ivanov, A., Comparative study of sol–gel and coprecipitated Ni–Al hydrotalcites. *J. Sol–Gel Sci. Technol.*, 2000, **19**, 453–457.
25. Prevot, V., Forano, C. and Besse, J. P., Syntheses and thermal and chemical behavior of tartrate and succinate intercalated Zn_3Al and Zn_2Cr layered double hydroxides. *Inorg. Chem.*, 1998, **37**, 4293–4301.
26. Vaysse, C., Guerlou-Demourgues, L. and Delmas, C., Thermal evolution of carbonate pillared layered hydroxides with (Ni, L) (L = Fe, Co) based slabs: grafting or nongrafting of carbonate anions. *Inorg. Chem.*, 2002, **41**, 6905–6913.
27. Reichle, W. T., Kang, S. Y. and Everhardt, D. S., The nature of the thermal decomposition of a catalytically active anionic clay mineral. *J. Catal.*, 1986, **101**, 352–359.
28. Sato, T., Fujita, H., Endo, T., Shimada, M. and Tsunashima, A., Synthesis of. hydrotalcite-like compounds and their physico-chemical properties. *React. Solids*, 1988, **5**, 219–228.
29. Stanimirova, T. and Kirov, G., Cation composition during recrystallization of layered double hydroxides from mixed (Mg, A1) oxides. *Appl. Clay Sci.*, 2003, **22**, 295–301.
30. Stanimirova, T., Kirov, G. and Dinolova, E., Mechanism of hydrotalcite regeneration. *J. Mater. Sci. Lett.*, 2001, **20**, 453–455.
31. Boclair, J. W. and Braterman, P. S., Layered double hydroxide stability. 1. Relative stabilities of layered double hydroxides and their simple counterparts. *Chem. Mater.*, 1999, **11**, 298–302.
32. Boclair, J. W. and Braterman, P. S., One-step formation and characterization of Zn(II)–Cr(III) layered double hydroxides, $Zn_2Cr(OH)_6X$ (X = Cl, SO_4). *Chem. Mater.*, 1998, **10**, 2050–2052.
33. Xu, Z. P. and Lu, G. Q., Hydrothermal synthesis of layered double hydroxides (LDHs) from mixed MgO and Al_2O_3: LDH formation mechanism. *Chem. Mater.*, 2005, **17**, 1055–1062.